

Antitumor activity of the water-soluble polysaccharide from *Hyriopsis cumingii* in vitro

Shuiqing Qiu, Shuling Huang, Juan Huang, Jianlin Pan and Weiyun Zhang
Toxicol Ind Health 2010 26: 151 originally published online 22 February 2010
DOI: 10.1177/0748233710362376

The online version of this article can be found at:
<http://tih.sagepub.com/content/26/3/151>

Published by:



<http://www.sagepublications.com>

Additional services and information for *Toxicology and Industrial Health* can be found at:

Email Alerts: <http://tih.sagepub.com/cgi/alerts>

Subscriptions: <http://tih.sagepub.com/subscriptions>

Reprints: <http://www.sagepub.com/journalsReprints.nav>

Permissions: <http://www.sagepub.com/journalsPermissions.nav>

Citations: <http://tih.sagepub.com/content/26/3/151.refs.html>

>> [Version of Record](#) - Mar 31, 2010

[OnlineFirst Version of Record](#) - Feb 22, 2010

[What is This?](#)

Antitumor activity of the water-soluble polysaccharide from *Hyriopsis cumingii* in vitro

Shuiqing Qiu¹, Shuling Huang¹, Juan Huang¹,
 Jianlin Pan² and Weiyun Zhang¹

Abstract

As a freshwater pearl mussel, *Hyriopsis cumingii* is widely cultured in China to produce pearls. This study was made to explore the antitumor activity of water-soluble polysaccharide (WSP) from mantles of *H. cumingii*. Cell viability of human hepatocarcinoma HepG2 cells was estimated by MTT method. Cell cycle analysis was determined by flow cytometry. Apoptosis was observed under fluorescence microscopy and confirmed by DNA fragment assay. Reverse transcriptase-polymerized chain reaction (RT-PCR) and immunocytochemistry were carried to evaluate *c-myc*, *bcl-2* and *cyclinD1* gene expressions in HepG2 cells. Furthermore, intracellular reactive oxygen species (ROS) production was assessed by flow cytometry. After WSP treatment, the growth of HepG2 cells was inhibited and most of cells arrested in G₀/G₁ phase ($p < .01$); apoptotic changes in nucleus and cytoplasm were also observed in WSP-treated cells; percentage of apoptotic rate significantly increased in a dose-dependent manner ($p < 0.001$); DNA fragmentation was detected in treated HepG2 cells; The mRNA level and protein level of *c-myc*, *bcl-2* and *cyclinD1* were decreased in the treated HepG2 cells. ROS was significantly increased in a dose- and time-dependent manner as well. The results suggested that WSP has potent antitumor activity.

Keywords

antitumor, apoptosis, cell cycle, *Hyriopsis cumingii*, polysaccharide

Introduction

Hyriopsis cumingii, belonging to the Unionidae family, is an endemic species of Chinese freshwater pearl mussels. It is of great economic importance and is widely cultivated in China to produce pearls, which are traditionally used as ornament and natural nutriment. Pearls are also excellent source of calcium and some trace metal elements that are beneficial to human health (Gao et al., 2008). Besides, mantles or visceral masses of *H. cumingii* have various nutritional components including polysaccharides as well (Zhou et al., 2006). However, in China, after pearls are harvested, mantles and visceral masses are usually discarded.

Bioactive polysaccharides have been found existing widely in medicinal fungi (Berović et al., 2003; Oka et al., 1996), plants (Chen et al., 2007; Leung et al., 1997; Tada et al., 2007) and mollusca (Volpi et al., 1998). So there is a promising research field for

discovering and evaluating polysaccharides from various kinds of organism with bioactive properties.

The main objective of this study was to investigate the bioactivity of water-soluble polysaccharide (WSP) from the mantle of *H. cumingii* and preliminarily confirm its antitumor activity. This might prompt to explore the potential economic value of *H. cumingii*.

¹ Jiangsu Key Laboratory of Molecular Medicine, Medical school, Nanjing University, Nanjing, P. R. China

² Freshwater Fisheries Research Institute of Jiangsu Province, Nanjing, P. R. China

Corresponding author:

Weiyun Zhang, Medical School of Nanjing University, Nanjing, 210093, China.

Email: zhangwy@nju.edu.cn

Materials and methods

Preparation of the WSP

H. cumingii was cultured in a local fish pond of the Hebei village, Yongning town, Pukou District, Nanjing, P. R. China for five years. After pearls were taken out, the mantles were collected immediately. The mantles were firstly homogenated by mechanical homogenizer and then extracted for 3 hours in distilled water at 100°C (the ratio of water to mantle tissue is 2:1). The mixture was centrifuged at 3000 rpm for 10 min to get the supernatant. The residue was extracted twice. The total supernatant was concentrated to a small volume. Three-time volume of 1.67% (w/v) cetyltrimethylammonium bromide (CTAB) solution was slowly added to the concentrated supernatant with continuous stirring at 4°C until a precipitate formed. The precipitate was washed with absolute ethanol and acetone alternately three times to remove lipid. After the solvents were volatilized, the precipitate was dissolved in distilled water, dialyzed, centrifuged and then the supernatant was freeze-dried to obtain the polysaccharide WSP powder. For cell culture, WSP was dissolved in the complete medium and then was sterilized by filtration.

Cell line and culture

Human hepatocellular carcinoma cell line (HepG2) was obtained from the cell bank in Shanghai and grown in RPMI 1640 medium containing 10% heat-inactivated fetal calf serum (Gibco) serum, penicillin (100 U/mL) and streptomycin (100 µg/mL). Cells were maintained at 37°C in a humidified 5% CO₂ atmosphere. Exponentially growing cells were collected for the experiments.

Detection of cell proliferation

Growth inhibitory effect of WSP on HepG2 cells was determined by measuring the absorbance of 3-(4,5-dimethylthiazol-2-yl)-2,5-diphenyltetrazoliumbromide (MTT) dye for living cells. Briefly, 8×10^3 cells in 80 µL per well were seeded in 96-well plates, and then added 80 µL of sterile WSP solution at final concentrations of 25 µg/mL, 50 µg/mL, 100 µg/mL and 200 µg/mL, respectively. After incubation for 24 hours, 48 hours and 72 hours, 10 µL of MTT (5 mg/mL, Sigma, St Louis, MO, USA) was added to each well and incubated for an additional 4 hours at 37°C. Then 80 µL of 20% (w/v) SDS was added into each well.

After incubation overnight at 37°C, the optical density was measured using a microplate reader (Bio-Tek ELX800, USA) at the wavelength of 570 nm.

Cell cycle analysis

For analyzing cycle-phase distribution, nuclear DNA of HepG2 cells was labeled with propidium iodide (PI) and estimated by flow cytometry. Firstly, cells (6×10^4) were seeded in 24-well plates and were treated with WSP for 48 hours at final concentrations of 25 µg/mL, 50 µg/mL, 100 µg/mL and 200 µg/mL, respectively. Cells were harvested and resuspended in phosphate buffered saline (PBS), and then fixed overnight at 4°C in 70% ethanol. After that, the cells were collected by centrifugation, suspended in 100 µL of PBS buffer containing 2% Triton X-100 (v/v) and 50 µg/mL RNase A and stained with PI (100 µg/mL) for 30 min at 4°C. Finally, the cells were analyzed with a FACS Calibur flow cytometer (Becton and Dickinson). A total of 10,000 cells from each sample were acquired and analyzed. The percentage of cells in each cell cycle phase was estimated by using the WinMDI 2.9 research software program.

Morphological observation of HepG2 cells by fluorescence microscopy

HepG2 cells (6×10^4) were seeded in 6-well plates. After 48 hours treatment with different concentrations of WSP, the cell viability was assessed by fluorescence microscopy staining using acridine orange and ethidium bromide (AO/EB; Ribble et al., 2005). Briefly, 10 µL of dye mixture (100 µg/mL AO and 100 µg/mL EB in PBS) was added to each well and mixed gently, and then the cells were checked under fluorescence microscopy. To determine the percentage of apoptotic cells, active and apoptotic cells were counted in 10 microscopic fields for each group.

DNA ladder detection

To examine nucleosomal fragments of HepG2 cells, DNA ladder assay was carried as previously described (Jenkins et al., 2001). HepG2 cells (1×10^6) were seeded in culture flasks. After 48 hours treatment with different concentrations of WSP, cells were collected and lysed in 250 µL of digestion buffer (0.4% Triton-X, 20 mM Tris, 0.4 mM EDTA) at 4°C for 15 min. After centrifugation at 13,000g for 5 min at 4°C, the supernatants were transferred into clean tubes. Nucleosomal fragments were precipitated overnight

with an equal volume of isopropanol after adjustment to 0.5 M NaCl. The precipitate was washed with 70% ethanol twice, dried slightly, and resuspended in 40 μ L of TE buffer (10 mM Tris-HCl, pH 8.0, 1 mM EDTA). Then, it was subjected to 1% agarose gel electrophoresis at 100 V for 15 min and was visualized under ultraviolet (UV) light and photographed.

mRNA levels of c-myc, bcl-2 and cyclinD1 detected by reverse transcriptase-polymerized chain reaction (RT-PCR)

Total RNA from HepG2 cells was isolated using Biozol reagent (BioFlux, Japan) and 2 μ g of total RNA was used to reverse-transcribe into cDNA according to the manufacturer's protocol (M-MLV RT, Promega, USA). PCR amplification was performed with 1 unit Taq polymerase (Fermentas) with a total volume of 25 μ L. The primers were as follows: c-myc forward 5'-TACATCCTGTCCGTC CAAGCA-3', reverse 5'-TCAGCCAAGGTTGTGAGGTTG-3'; bcl-2 forward 5'-TCCCTCGCTGCACAAATACTC-3', reverse 5'-TTCTGCCCTGCCAAATCT-3'; cyclinD1 forward 5'-TGGAGGTCTGCGAGGAACAGAA-3', reverse 5'-TGCAGGCGGCTCTTTTCA-3'. β -actin was used as the internal standard. Its primers were the same as previous report (Zhang et al., 2008). The PCR conditions consisted of an initial step at 95°C for 5 min, followed by 30 cycles of 95°C for 30 sec, 58°C for 40 sec and 72°C for 40 sec. The last cycle was followed by an additional extension incubation of 10 min at 72°C. The amplified PCR products were subjected to 1% agarose gels, and then photographed by a digital scanning system.

Protein expression of c-myc, bcl-2 and cyclinD1 detected by immunocytochemistry

Immunocytochemical method was used to estimate the expressions of c-myc, bcl-2 and cyclinD1. 3.0×10^4 cells were cultured on the coverslips in 6-well plates. After treated with different concentrations of WSP for 48 hours, cells were washed with PBS and fixed with ice-cold 80% acetone at 4°C for 15 min. Then cells were pretreated with 3% H₂O₂ for 10 min to remove the endogenous peroxidase. Following washes in PBS three times, the cells were incubated in 5% bovine serum albumin for 30 min. Then the cells were incubated in a wet chamber with a polyclonal rabbit antibody at 37°C for 1 hour. Anti-c-myc, anti-bcl-2 and anti-cyclinD1 IgG antibody was

applied at a 1:200 dilution. After washing in PBS three times, the cells were incubated with biotinylated secondary antibody (biotin-goat anti-rabbit IgG) at 37°C for 30 min. After washing again, they were treated with streptavidin peroxidase for 20 min. Then they were incubated with DAB (3,3'-diaminobezidine as a substrate for staining) solution for 5 min. Finally, the reaction was stopped with distilled water. A positive reaction was characterized by dark brown staining in the nucleus and/or cytoplasm. Under microscopic field at $\times 400$ magnification, positive and negative cells were counted in 10 fields for each group. The positive cell percentage was calculated.

Assessment of intracellular reactive oxygen species (ROS) production

Dichlorofluorescein diacetate (DCFH-DA; Sigma) was used as a substrate for measuring intracellular ROS. This nonfluorescent molecule may be oxidized by cellular oxidants to a highly fluorescent compound, dichlorofluorescein (DCF), which is unable to leave the cells. In this study, cells were cultured with various concentrations of WSP (25 μ g/mL, 50 μ g/mL, 100 μ g/mL and 200 μ g/mL). After 3 hours, 6 hours, 12 hours, 24 hours treatment, cells were incubated with 5 μ M DCFH-DA for 30 min at room temperature in the dark. Intracellular fluorescence was measurable by flow cytometry and analyzed with WinMDI 2.9 software.

Statistical analysis

Data are expressed as mean \pm SD. They were evaluated by the one-way analysis of variance (ANOVA), followed by Student's *t* test. $p < 0.05$ was considered statistically significant.

Results

Effects of WSP on proliferation of HepG2 cells

We examined the effect of WSP on the proliferation of human hepatoma cells by using MTT assay. As shown in Table 1, significant inhibition of proliferation produced as early as 24 hours after cells were treated with WSP at all the four concentrations when compared with control ($p < 0.05$). Moreover, the same inhibition effect was observed after 48 hours treatment by WSP ($p < 0.05$ or $p < 0.01$). However, when cells were treated for 72 hours, only 200 μ g/mL of WSP showed significant inhibition ($p < 0.05$).

Table 1. Effects of water-soluble polysaccharide (WSP) on proliferation of HepG2 cells

Concentration ($\mu\text{g/mL}$)	$A_{570 \text{ nm}}$		
	24 hours	48 hours	72 hours
0	0.6090 \pm 0.0230	0.9087 \pm 0.0392	1.3612 \pm 0.1041
25	0.5973 \pm 0.0184 ^a	0.8487 \pm 0.0357 ^a	1.2702 \pm 0.1541
50	0.5912 \pm 0.0208 ^a	0.8167 \pm 0.0423 ^b	1.2950 \pm 0.0842
100	0.5835 \pm 0.0337 ^a	0.8053 \pm 0.0438 ^b	1.2725 \pm 0.0723
200	0.5815 \pm 0.0354 ^a	0.7993 \pm 0.0527 ^b	1.1895 \pm 0.1505 ^a

^a $p < 0.05$, compared with control group, $n = 6$.

^b $p < 0.01$, compared with control group, $n = 6$.

Table 2. Effects of water-soluble polysaccharide (WSP) on cell cycle-phase distribution of HepG2 cells

Concentration ($\mu\text{g/mL}$)	G_0/G_1	S	G_2/M
0	42.42 \pm 2.45	7.80 \pm 0.79	50.00 \pm 3.07
25	46.34 \pm 3.98	9.02 \pm 0.10	44.90 \pm 4.74
50	47.15 \pm 1.03 ^a	8.29 \pm 0.83	44.84 \pm 1.23 ^a
100	49.41 \pm 3.78 ^a	9.00 \pm 0.54	41.85 \pm 4.04 ^a
200	51.31 \pm 4.07 ^a	8.89 \pm 0.18	39.99 \pm 4.01 ^a

^a $p < 0.01$, compared with control group, $n = 6$.

Effects of WSP on cell cycle-phase distribution

Cell cycle distribution of HepG2 cells was determined by flow cytometry. WSP significantly caused HepG2 cells arrest at G_0/G_1 phase and decreased the cell population of G_2/M phase at doses of 50 $\mu\text{g/mL}$, 100 $\mu\text{g/mL}$ and 200 $\mu\text{g/mL}$ ($p < 0.01$) after 48 hours treatment (Table 2).

Effects of WSP on morphological changes of HepG2 cells

To investigate whether the growth-inhibitory effect of WSP was related to the induction of apoptosis, the DNA-binding fluorescent dyes AO and EB along with fluorescence microscopy was used. Live cells fluoresce green (with acridine orange) and apoptotic cells fluoresce orange (with ethidium bromide). As shown in Figure 1, control cells contained a nucleus with organized chromatin structure, an intact cytoplasm and a normal green nucleus (Figure 1a). In contrast, morphological changes in nucleus and cytoplasm were observed in WSP-treated cells, especially in cells treated with 100 $\mu\text{g/mL}$ and 200 $\mu\text{g/mL}$ of WSP (Figure 1d and e). They presented the typical apoptotic features: chromatin condensation and nuclear fragmentation. Also, membrane-bound apoptotic bodies compacted cytoplasmic organelles and/or nuclear

fragments can be observed. Moreover, percentage of apoptotic cells in WSP-treated groups was significantly higher than that of controls ($p < 0.001$; Table 3).

DNA ladder

DNA fragmentation is a typical feature of apoptosis. As shown in Figure 2, WSP at 50 $\mu\text{g/mL}$, 100 $\mu\text{g/mL}$ and 200 $\mu\text{g/mL}$ caused significant DNA fragmentation, and observed DNA 'ladders' by agarose gel electrophoresis. The results indicated that 50, 100, 200 $\mu\text{g/mL}$ of WSP induced apoptosis in HepG2 cells. This is consistent with AO/EB and PI staining experiments.

Effects of WSP on *c-myc*, *bcl-2* and *cyclinD1* mRNA levels

We monitored the mRNA expression of *c-myc*, *bcl-2* and *cyclinD1* genes in WSP-treated HepG2 cells by RT-PCR. The amplified products were checked by agarose gel electrophoresis. The product sizes of *c-myc*, *bcl-2* and *cyclinD1* and β -actin (internal standard) were 200 bp, 124 bp, 106 bp and 389 bp, respectively (Figure 3a). The densitometric ratio of the corresponding bands was calculated for each sample shown in Figure 3b. The data demonstrates that WSP at 100 $\mu\text{g/mL}$ and 200 $\mu\text{g/mL}$ doses

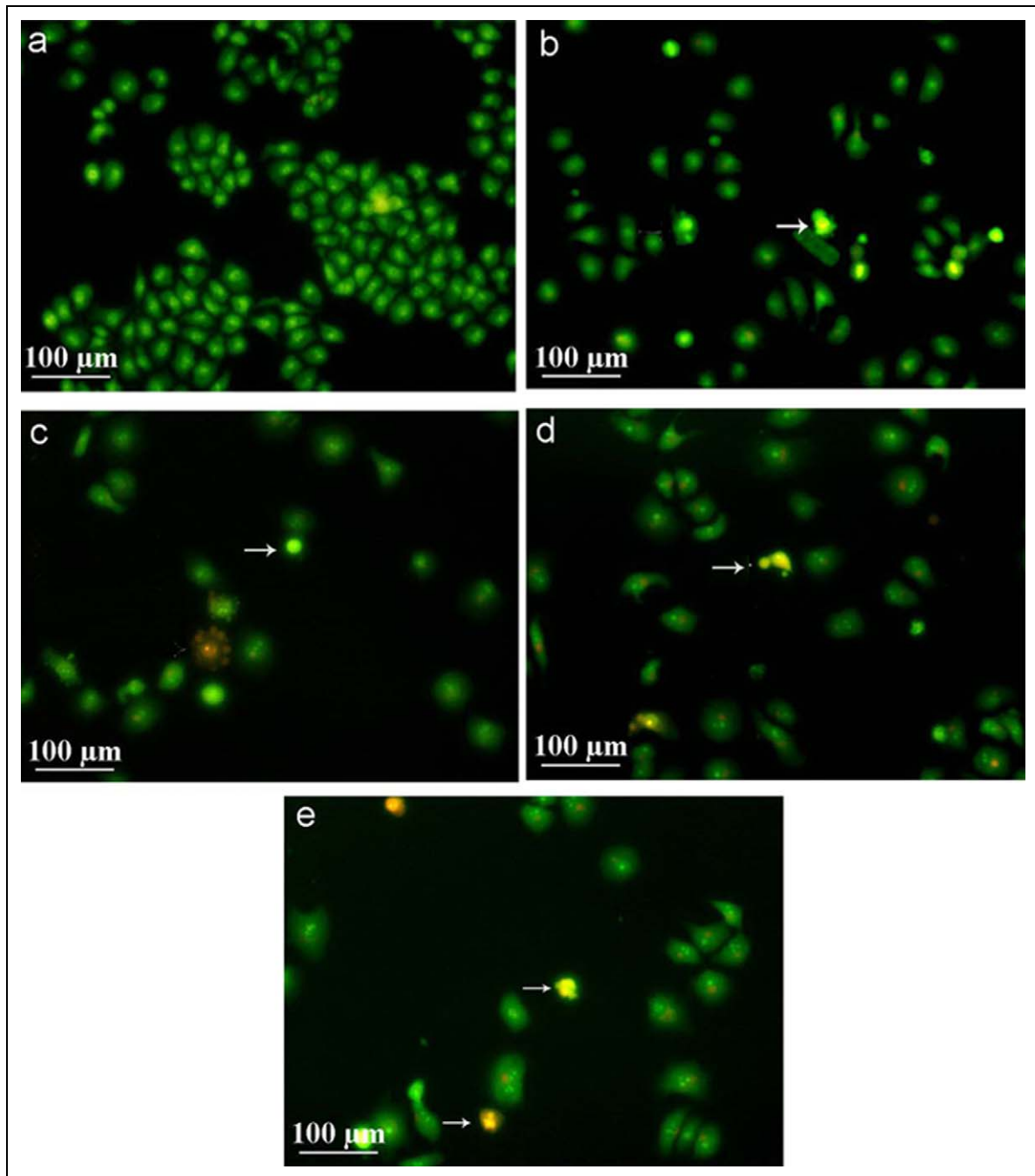


Figure 1. Morphological changes of water-soluble polysaccharide (WSP)-treated HepG2 cells stained with acridine orange and ethidium bromide (AO/EB; magnification, $\times 200$). The arrows point at apoptotic cells; (a) control; (b) 25 $\mu\text{g}/\text{mL}$; (c) 50 $\mu\text{g}/\text{mL}$; (d) 100 $\mu\text{g}/\text{mL}$; (e) 200 $\mu\text{g}/\text{mL}$.

significantly inhibited the mRNA expression of *c-myc* when compared to control group ($p < 0.05$); WSP at 25 $\mu\text{g}/\text{mL}$, 50 $\mu\text{g}/\text{mL}$, 100 $\mu\text{g}/\text{mL}$ and 200 $\mu\text{g}/\text{mL}$ doses significantly decrease the mRNA level of *bcl-2* ($p < 0.05$); WSP at 50, 100, 200 $\mu\text{g}/\text{mL}$ significantly declined the mRNA level of *cyclinD1* ($p < 0.05$).

Effects of WSP on c-myc, bcl-2 and cyclinD1 protein expression

The protein expressions of *c-myc*, *bcl-2* and *cyclinD1* in WSP-treated HepG2 cells were analyzed using immunocytochemical method. Typical positive products of *c-myc* were brown yellow granules both in the

Table 3. Apoptotic rate of HepG2 cells observed by fluorescence microscopy after acridine orange and ethidium bromide (AO/EB) staining

Concentration ($\mu\text{g/mL}$)	Apoptotic rate (%)
0	2.20 ± 0.83
25	5.95 ± 2.48^a
50	9.01 ± 5.30^a
100	12.61 ± 5.57^a
200	13.98 ± 7.24^a

^a $p < 0.001$, compared with control group, $n = 6$.

cytoplasm and nucleus (Figure 4a–e), while the positive products of bcl-2 were brown yellow granules mainly in the cytoplasm (Figure 4f–j), and the positive products of cyclinD1 were brown yellow granules both in the cytoplasm and nucleus (Figure 4k–o).

Taking brown particles intracellular as positive, we counted the rate of positive cells in 10 fields randomly and compared them with control group, which was not exposed to WSP. As shown in Table 4, WSP at dose of 100 $\mu\text{g/mL}$ and 200 $\mu\text{g/mL}$ significantly reduced the protein expression of c-myc and cyclinD1 ($p < 0.05$ or $p < 0.01$); WSP at dose of 50 $\mu\text{g/mL}$, 100 $\mu\text{g/mL}$ and 200 $\mu\text{g/mL}$ significantly declined the protein expression of bcl-2 ($p < 0.05$ or $p < 0.01$).

Measurement of WSP-induced ROS in HepG2 cells

HepG2 cells were treated with indicated concentrations of WSP for 3 hours, 6 hours, 12 hours and 24 hours and stained with DCFH-DA. The levels of ROS were in direct ratio to the fluorescent intensity of DCF. As shown in Figure 5, the first curve represents the control, the second curve represents the WSP-treated cells. The result revealed that WSP significantly induced increase of ROS in a dose- and time-dependent manner.

Discussion

The results showed that WSP inhibited HepG2 cell viability and induced their G_0/G_1 phase arrest. DNA degradation and condensation were the first-steps of biochemical features of apoptosis (Arends et al., 1990; Arends et al., 1991). We observed HepG2 cells apoptosis with nuclear chromatin concentration and fragmentation as well as the formation of apoptotic bodies under fluorescence microscope. The hallmark of apoptotic cell death is reflected by the degradation of genomic DNA in characteristic discontinuous

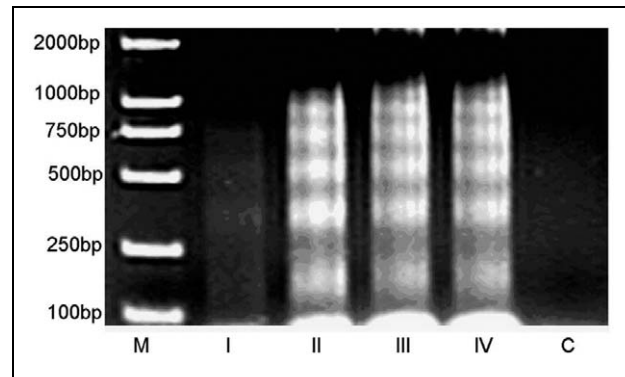


Figure 2. DNA fragments in water-soluble polysaccharide (WSP)-treated HepG2 cells analyzed by agarose gel electrophoresis. M stands for DNA marker, C stands for control, I–IV stand for 25 $\mu\text{g/mL}$, 50 $\mu\text{g/mL}$, 100 $\mu\text{g/mL}$, 200 $\mu\text{g/mL}$ of WSP-treated cells.

“ladder-like” fragments (López Nigro et al., 2008). This result indicated that the decrease in cell viability by WSP in the present study was due to induction of apoptosis.

To address the mechanism of apoptosis induced by WSP, we further investigated the expression of genes involved in regulation of cell proliferation. Proto-oncogene c-myc is a driving signal for cell proliferation, cell cycle progression, growth, oncogenic transformation and angiogenesis (Adhikary and Eilers, 2005; Cowling and Cole, 2006; Ma et al., 2008). Its overexpression has been implicated in the development and progression of many human cancers (Levens 2003; Yang et al., 2005). Inhibition of c-myc sometimes causes a proliferative arrest of human tumor cells (Biroccio et al., 2003). In our study, growth inhibition of HepG2 cells was observed after cells treated with WSP, in the same time, expression of c-myc in HepG2 was significantly decreased.

Bcl-2 protein has also been identified to play an essential role in the apoptotic response. It is an intracellular membrane-associated protein that can prevent cell death induced by a variety of apoptotic stimuli (Park et al., 1997) and it overexpresses in a variety of human tumors (Herrmann et al., 1997). Down-regulation of bcl-2 can direct cells to a kind of death, which shares several aspects with the apoptotic program (Sirchia et al., 2008). The present study demonstrated that bcl-2 expression markedly decreased in WSP-treated HepG2 cells. This means WSP could lead to the proliferation inhibition and apoptosis of HepG2 by regulating bcl-2 expression as well.

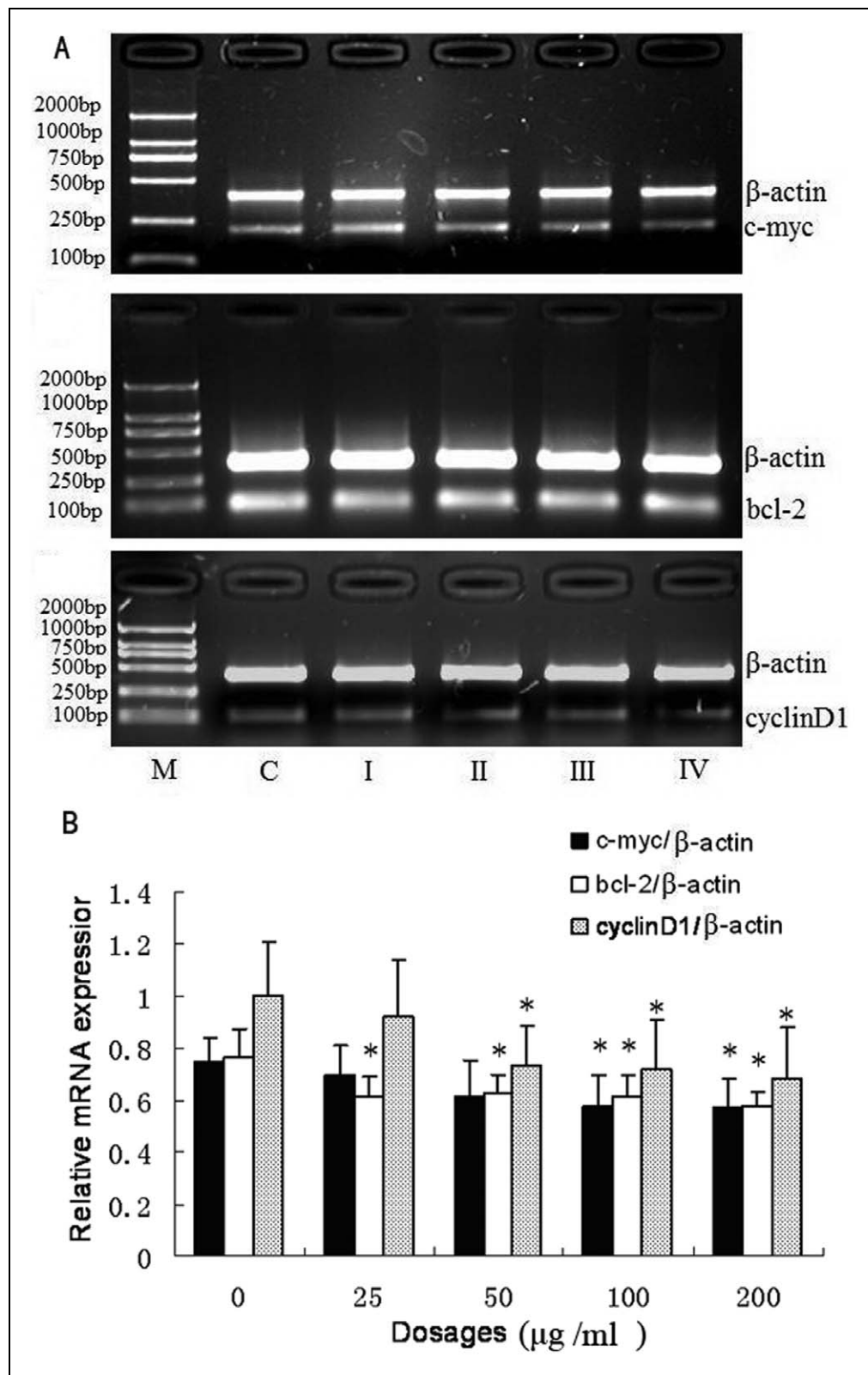


Figure 3. Expressions of c-myc, bcl-2 and cyclinD1 mRNA in water-soluble polysaccharide (WSP)-treated HepG2 cells analyzed by reverse transcriptase-polymerized chain reaction (RT-PCR; a, RT-PCR products of the c-myc, bcl-2 and cyclinD1, C stands for control, I-IV stand for 25 μg/mL, 50 μg/mL, 100 μg/mL, 200 μg/mL of WSP-treated cells; (b) The relative intensity of c-myc, bcl-2 and cyclinD1 mRNA compared to β-actin mRNA, * $p < 0.05$, compared with control group, $n = 6$.

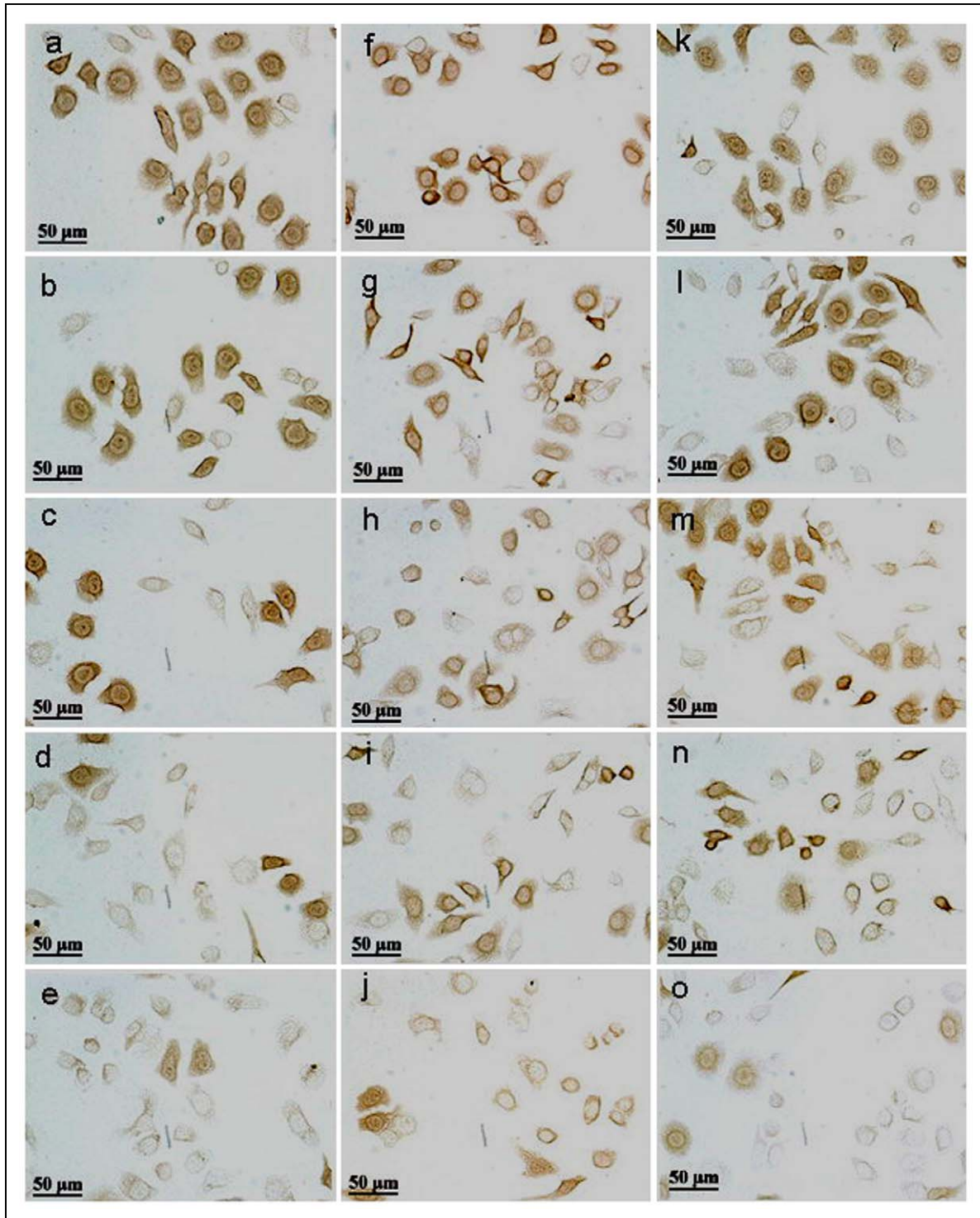


Figure 4. Protein expressions of c-myc, bcl-2 and cyclinD1 in water-soluble polysaccharide (WSP)-treated HepG2 cells detected by immunocytochemistry (magnification, $\times 400$); (a–e) c-myc staining of HepG2 cells treated with 0 (control), 25, 50, 100 and 200 $\mu\text{g}/\text{mL}$ of WSP; (f–j) bcl-2 staining of HepG2 cells treated with 0 (control), 25, 50, 100 and 200 $\mu\text{g}/\text{mL}$ of WSP; (k–o) cyclinD1 staining of HepG2 cells treated with 0 (control), 25, 50, 100 and 200 $\mu\text{g}/\text{mL}$ of WSP.

We also determined whether WSP treatment can influence the level of the cell cycle regulatory protein cyclinD1 in view of that the HepG2 cells arrested in

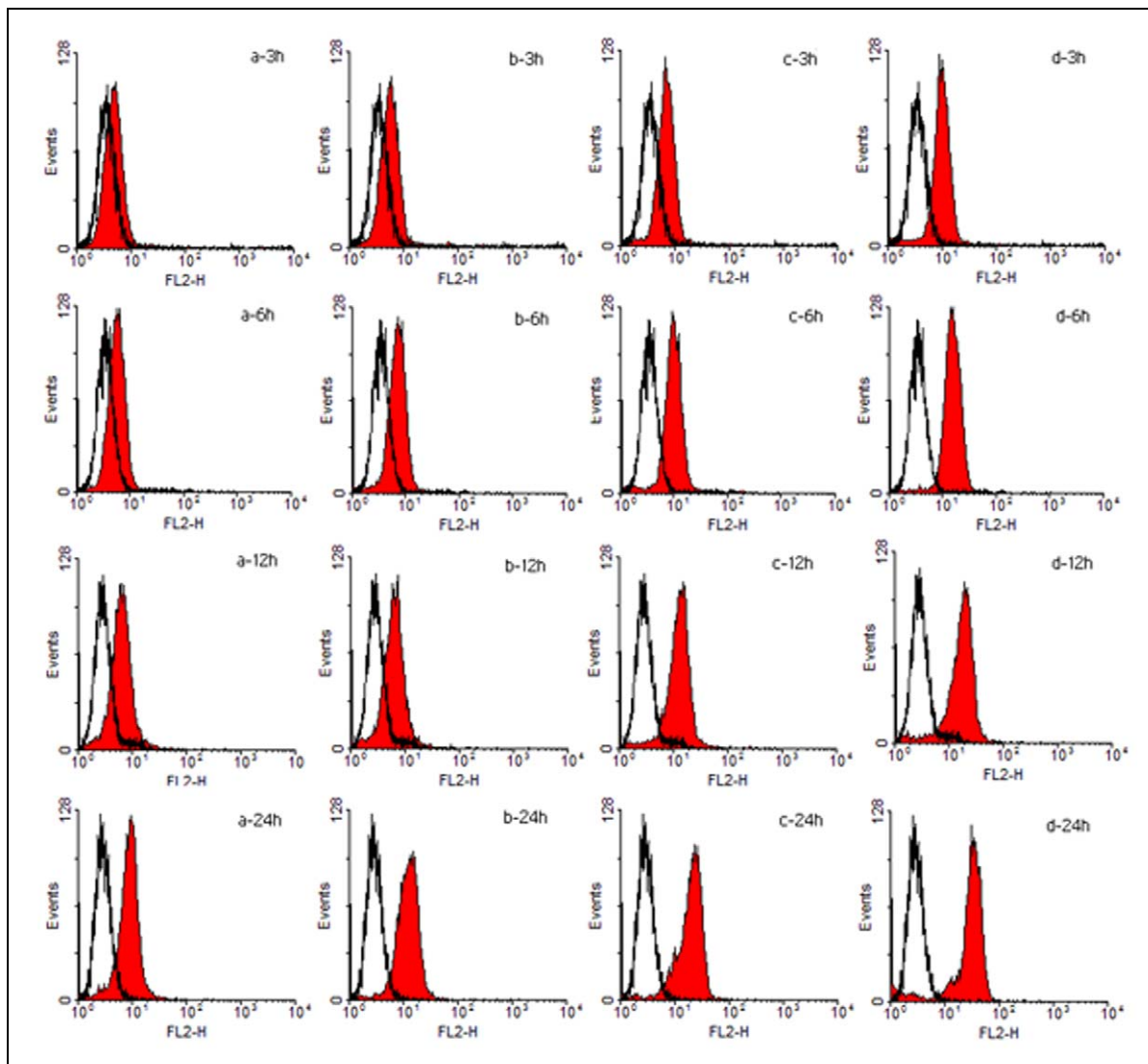
G_0/G_1 phase after treatment. This observation indicates that the level of cyclinD1 expression was down-regulated significantly in a dose-dependent

Table 4. Positive cell percentage of c-myc, bcl-2 and cyclinD1 in HepG2 cells treated with water-soluble polysaccharide (WSP)

Concentration ($\mu\text{g/mL}$)	c-myc Positive percentage (%)	bcl-2 Positive percentage (%)	cyclinD1 positive percentage (%)
0	55.51 ± 0.12	59.46 ± 0.17	59.14 ± 0.14
25	53.31 ± 0.16	57.59 ± 0.15	55.01 ± 0.11
50	46.01 ± 0.17	43.37 ± 0.09^a	49.22 ± 0.13
100	39.09 ± 0.16^a	41.21 ± 0.17^a	41.51 ± 0.17^a
200	38.84 ± 0.20^a	28.81 ± 0.21^b	35.60 ± 0.16^b

^a $p < 0.05$, compared with control group, $n = 10$.

^b $p < 0.01$, compared with control group, $n = 10$.

**Figure 5.** Effects of water-soluble polysaccharide (WSP) on intracellular peroxide levels measured using DCFHDA dye by flow cytometry. (a) 25 $\mu\text{g/mL}$ (b) 50 $\mu\text{g/mL}$, (c) 100 $\mu\text{g/mL}$ and (d) 200 $\mu\text{g/mL}$.

manner. Thus, WSP arrest cell proliferation in G₀/G₁ phase by probably suppressing the expression level of cyclinD1 in HepG2 cells.

Apoptosis can be initiated by a variety of stimuli, including chemotherapeutic agents, ionizing radiation, oxidants, and so on. Free radicals, particularly ROS, have been proposed as common mediators for apoptosis (Engel and Evans, 2006; Ozben, 2007). Exposure of cancer cells to ROS-generating agents exhaust the cellular antioxidant capacity, and a ROS level beyond a threshold leads to apoptosis. In our experiment, after treatment of WSP for 3 hours, 6 hours, 12 hours, 24 hours, HepG2 cells' ROS generation increases in a time- and dose-dependent manner, these results indicated that increase of ROS production took part in WSP-induced apoptosis of HepG2 cells.

In summary, we have shown that WSP inhibited the growth of human hepatocarcinoma cells by inducing G₀/G₁ arrest and apoptosis, with reduced mRNA and protein levels of c-myc, bcl-2 and cyclinD1 and increase of ROS generation. This report might provide us a new application of *H. cumingii* and explore more medicinal value of it.

Acknowledgement

This work was financed by the National Nature Science Foundation of China (No. 30873188 to Weiyun Zhang).

References

- Adhikary S, Eilers M (2005) Transcriptional regulation and transformation by Myc proteins. *Nature Reviews Molecular Cell Biology* 6: 635–645.
- Arends MJ, Morris RG, and Wyllie AH (1990) Apoptosis: the role of the endonuclease. *American Journal of Pathology* 136: 593–608.
- Arends MJ, Wyllie AH (1991) Apoptosis: mechanisms and roles in pathology. *International Review of Experimental Pathology* 32: 223–254.
- Berovič M, Habijanič J, Zore I, Wraber B, Hodžar D, Boh B, et al. (2003) Submerged cultivation of *Ganoderma lucidum* biomass and immunostimulatory effects of fungal polysaccharides. *Journal of Biotechnology* 103: 77–86.
- Biroccio A, Amodei S, Antonelli A, Benassi B, and Zupi G. (2003) Inhibition of c-Myc oncoprotein limits the growth of human melanoma cells by inducing cellular crisis. *Journal of Biological Chemistry* 278: 35693–35701.
- Chen W, Zhao Z, Chen S, and Li Y (2007) Optimization for the production of exopolysaccharide from *Fomes fomentarius* in submerged culture and its antitumor effect in vitro. *Bioresource Technology* 99: 3187–3194.
- Cowling VH, Cole MD (2006) Mechanism of transcriptional activation by the Myc oncoproteins. *Seminars in Cancer Biology* 16: 242–252.
- Engel RH, Evens AM. (2006) Oxidative stress and apoptosis: A new treatment paradigm in cancer. *Frontiers in Bioscience* 11: 300–312.
- Gao H, Chen H, Chen W, Tao F, Zheng Y, Jiang Y, et al. (2008) Effect of nanometer pearl powder on calcium absorption and utilization in rats. *Food Chemistry* 109: 493–498.
- Herrmann JL, Menter DG, Beham A, Von Eschenbach A, and McDonnell TJ (1997) Regulation of lipid signaling pathways for cell survival and apoptosis by bcl-2 in prostate carcinoma cells. *Experimental Cell Research* 234: 442–451.
- Jenkins JK, Suwannaroj S, Elbourne KB, Ndebele K, and McMurray RW (2001) 17- β -estradiol alter Jurkat lymphocyte cell cycling and induces apoptosis through suppression of Bcl-2 and cyclin A. *International Immunopharmacology* 1: 1897–1911.
- Levens DL (2003) Reconstructing MYC. *Gene Development* 17: 1071–1077.
- Leung M, Fung K, and Choy Y (1997) The isolation and characterization of an immunomodulatory and anti-tumor polysaccharide preparation from *Flammulina velutipes*. *Immunopharmacology* 35: 255–263.
- López Nigro MM, Carballo MA (2008) Genotoxicity and cell death induced by tinidazole (TNZ). *Toxicology Letters* 180: 46–52.
- Ma Y, Ou T, Hou J, Lu Y, Tan J, Gu L, et al. (2008) 9-*N*-Substituted berberine derivatives: stabilization of G-quadruplex DNA and down-regulation of oncogene c-myc. *Bioorganic and Medicinal Chemistry* 16: 7582–7591.
- Oka M, Hazama S, Suzuki M, Wang F, Wadamori K, Iizuka N, et al. (1996) In vitro and in vivo analysis of human leukocyte binding by the antitumor polysaccharide, lentinan. *International Journal of Immunopharmacology* 18: 211–216.
- Ozben T (2007) Oxidative stress and apoptosis: impact on cancer therapy. *Journal of Pharmacy Science* 96: 2181–2196.
- Park J, Kim I, Oh YJ, Lee K, Han PL, and Choi EJ (1997) Activation of c-Jun N-terminal kinase antagonizes an anti-apoptotic action of Bcl-2. *Journal of Biological Chemistry* 272: 16725–16728.
- Ribble D, Goldstein NB, Norris DA, and Shellman YG (2005) A simple technique for quantifying apoptosis in 96-well plates. *BMC Biotechnology* 5: 12.
- Sirchia R, Longo A, and Luparello C (2008) Cadmium regulation of apoptotic and stress response genes in tumoral

- and immortalized epithelial cells of the human breast. *Biochimie* 90: 1578–1590.
- Tada R, Harada T, Nagi-Miura N, Adachi Y, Nakajima M, Yadomae T, et al. (2007) NMR characterization of the structure of a β -(1 \rightarrow 3)-D-glucan isolate from cultured fruit bodies of *Sparassis crispa*. *Carbohydrate Research* 342: 2611–2618.
- Volpi N, Dondi M, and Bolognani AMF (1998) Characterization of a small chondroitin sulfate proteoglycan isolated from the mucus surrounding the embryos of *Viviparus ater* (Mollusca Gastropoda). *Biochimica et Biophysica Acta* 1380: 239–248.
- Yang G, Timme T, Frolov A, Wheeler T, and Thompson T (2005) Combined c-Myc and Caveolin-1 expression in human prostate carcinoma predicts prostate carcinoma progression. *Cancer* 103: 1186–1194.
- Zhang W, Li J, Qiu S, Chen J, and Zheng Y (2008) Effects of the exopolysaccharide fraction (EPSF) from a cultivated *Cordyceps sinensis* on immunocytes of H22 tumor bearing mice. *Fitoterapia* 79: 168–173.
- Zhou H, Liu Z, Li B, Li Y, Li J, and Su Y (2006) Nutritional components analysis of *Hyriopsis cumingii* meat and mantle after harvest of pearls. *Science and Technology of Food Industry* 27: 170–173. (in Chinese).

